Supplementary information

Improved electron-hole separation and migration in anatase TiO_2 nanorod/reduced graphene oxide composites and their significance on photocatalytic performance

Gregor Žerjav[a,*], Muhammad Shahid Arshad[a], Petar Djinović[a], Ita Junkar[b], Janez Kovač[b], Janez Zavašnik[c], Albin Pintar[a]

[a]Department for Environmental Sciences and Engineering, National Institute of Chemistry, Hajdrihova 19, SI-1001 Ljubljana, Slovenia

[b]Department of Surface Engineering and Optoelectronics, Jožef Stefan Institute, Jamova 39, SI-1000 Ljubljana, Slovenia

[c]Centre for Electron Microscopy and Microanalysis, Jožef Stefan Institute, Jamova 39, SI-1000 Ljubljana, Slovenia

[*]Corresponding author. Tel.: +386 1 47 60 249, fax: +386 1 74 60 460. *E-mail address:* gregor.zerjav@ki.si (G. Žerjav).

N_2 physisorption results

The nitrogen sorption isotherms and the corresponding pore size distribution curves for pure TiO_2 and TiO_2+rGO composites are presented in Fig. S1. According to IUPAC classification [1], all composites correspond to type IV isotherms which are typical for mesoporous materials with pore sizes in the range from 2 to 50 nm. Typical for type IV isotherms is a hysteresis loop (type H3), which is associated with the occurrence of N_2 condensation in pores. The hysteresis loops approach $P/P_0=1$ in a way, which suggests the presence of macropores in investigated samples (>50 nm). From the BJH pore size distribution plots presented in Figs. S1b and S1d we can see that the pore size distribution is not effected with the increasing rGO loading regardless of the type of TiO_2 for synthesizing composites.

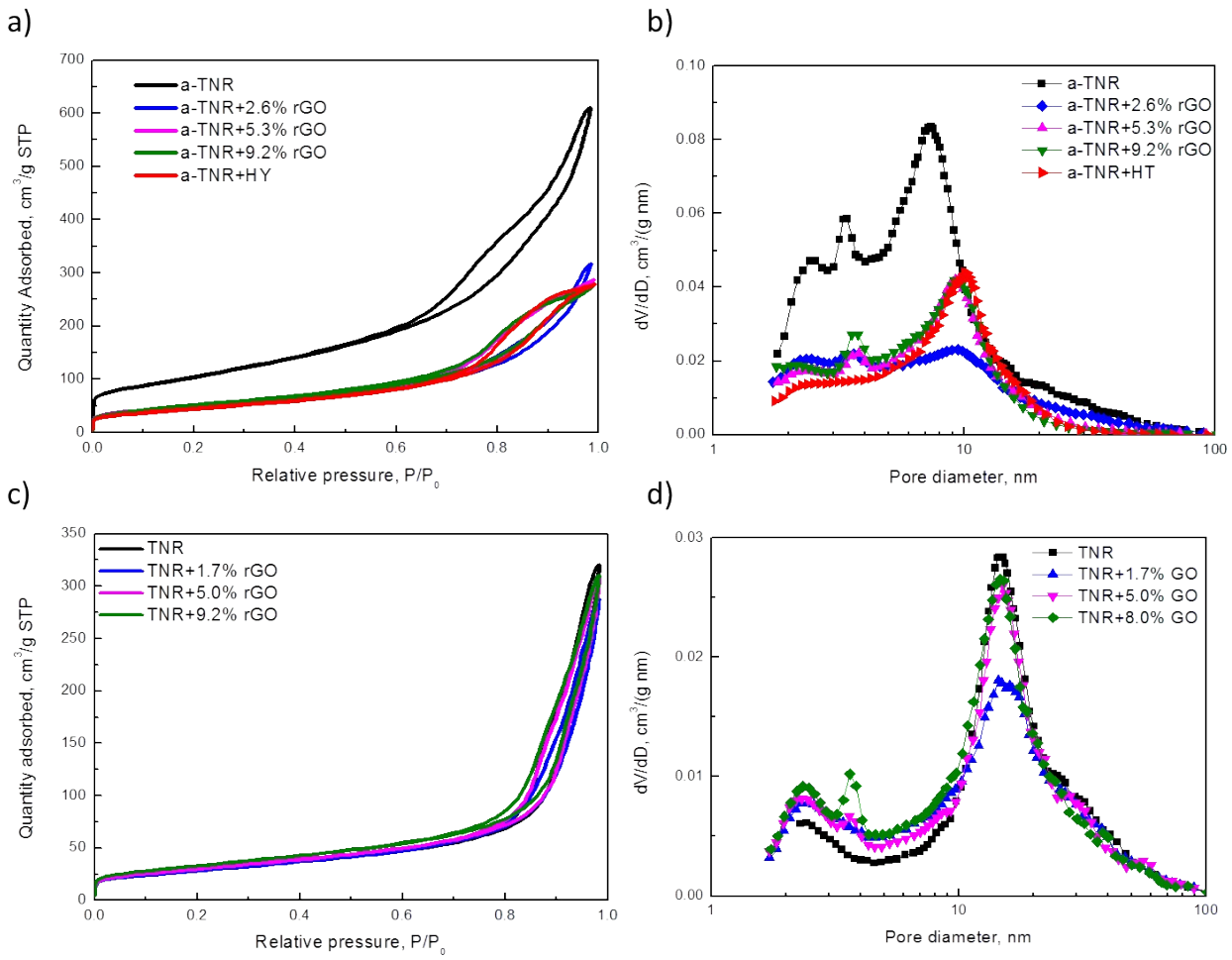

Fig. S1. N_2 adsorption-desorption isotherms and BJH pore size distributions of (a,b) a-TNR+rGO composites and (c,d) TNR+rGO composites with different rGO loadings.

Quantification of rGO content in the TNR+rGO composites

The CHNS elemental analysis of pure GO has shown that the content of C is 42.4 wt. %, which implies that in the composites with 4, 10 and 20 wt. % of nominal GO loading, 1.7, 4.2 and 8.4 wt. % belongs to C.

We performed TPO-MS analysis of a-TNR+9.2% rGO composite in order to investigate in detail combustion of the rGO phase and determine the temperature range where mass loss can be attributed to rGO oxidation. As one can see in Fig. S2, formation of CO as a result of the sample being exposed to diluted 5 % O_2/He stream is negligible in the entire temperature range examined. Desorption of H_2O takes place in two overlapping peaks, the first one centered at 70 and the second one at 220 ^oC, which decays slowly and reaches the baseline value at 630 ^oC. The low temperature peak likely originates from desorbed water, while the second one is attributed to thermal degradation and desorption of surface hydroxyl groups exhibiting a broad distribution of binding strengths. Desorption of CO_2 which indicates oxidation of rGO layers initiates at temperatures above 100 ^oC. The first small peak is centered at 200 ^oC. The CO_2 signal continues to rise at higher temperatures reaching the second, most intensive maximum at 590 ^oC. Afterwards, the CO_2 signal drops quickly to the baseline value at 630 ^oC. The O_2 signal is showing maxima in its consumption at the exact same positions at which peaks occur in the CO_2 signal. This indicates that CO_2 formation and O_2 consumption are directly linked and that CO_2 evolution is not a consequence of surface carbonate species decomposition, which would not require the presence of O_2. The obtained results provide the basis for attributing mass loss at temperatures below 340 ^oC to catalyst dehydroxylation and water desorption, whereas mass loss above 340 ^oC primarily originates from gasification of reduced GO. The mass losses in the composites obtained in the temperature range from 340 to 800 ^oC provide an evidence that rGO was successfully reduced during the hydrothermal procedure.

To analyze the actual composition of prepared TiO_2+rGO composites, TGA measurements in air were conducted. Figs. S3a and S3b show TGA curves obtained for a-TNR and TNR composites containing different amounts of rGO; the TGA curve for pure GO is illustrated, too. It can be seen that in the case of pure GO major weight loss occurs at around 180 ^oC because of pyrolysis of oxygen containing groups; as a result, CO, CO_2 and H_2O are produced [2]. GO was completely decomposed at temperatures above 680 ^oC. In the TGA curves belonging to TiO_2+rGO composites we can observe that there is a weight loss at around 150-180 ^oC, and the second one in the range of 340-650 ^oC. No weight loss was observed above 650 ^oC. The residual mass remaining at 800 ^oC is associated with the TiO_2 phase in the composites; we can see that with the increasing rGO loading in the composites, the residual masses are decreasing due to lower content of TiO_2. If we compare the weight losses of the composites between 340 and 800 ^oC, we can see that the mass losses in this temperature range increase with the increasing GO loading: in the case of TNR composites from 1.7, 5 and 8 % for composites with 4, 10 and 20 wt. % of nominal GO loading, and 2.6, 5.3 and 9.2 % for a-TNR composites with 4, 10 and 20 wt. % of nominal GO loading, respectively. These values are in rather good agreement with the TGA data reported above concerning the loss of mass in the temperature range of 340-800 ^oC.

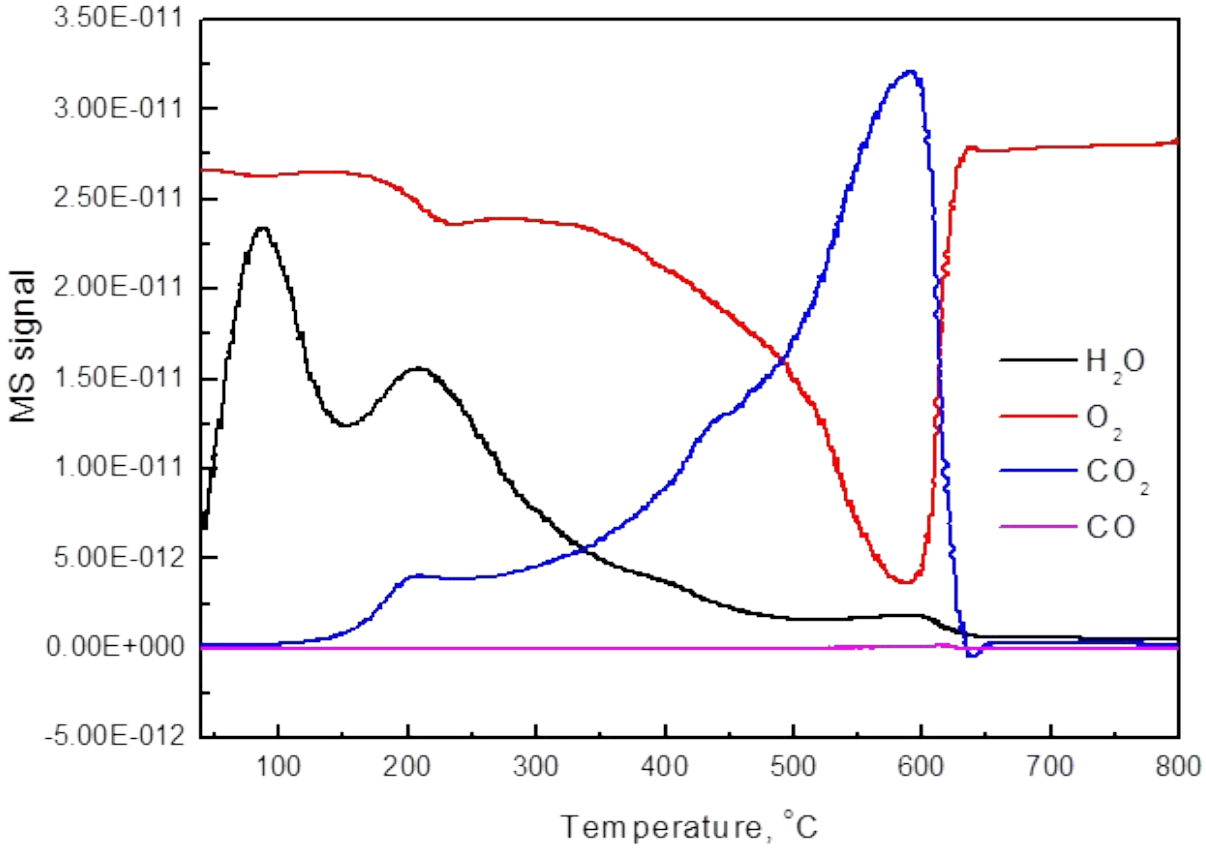

Fig. S2. TPO-MS analysis of TNR+8.0% rGO sample.

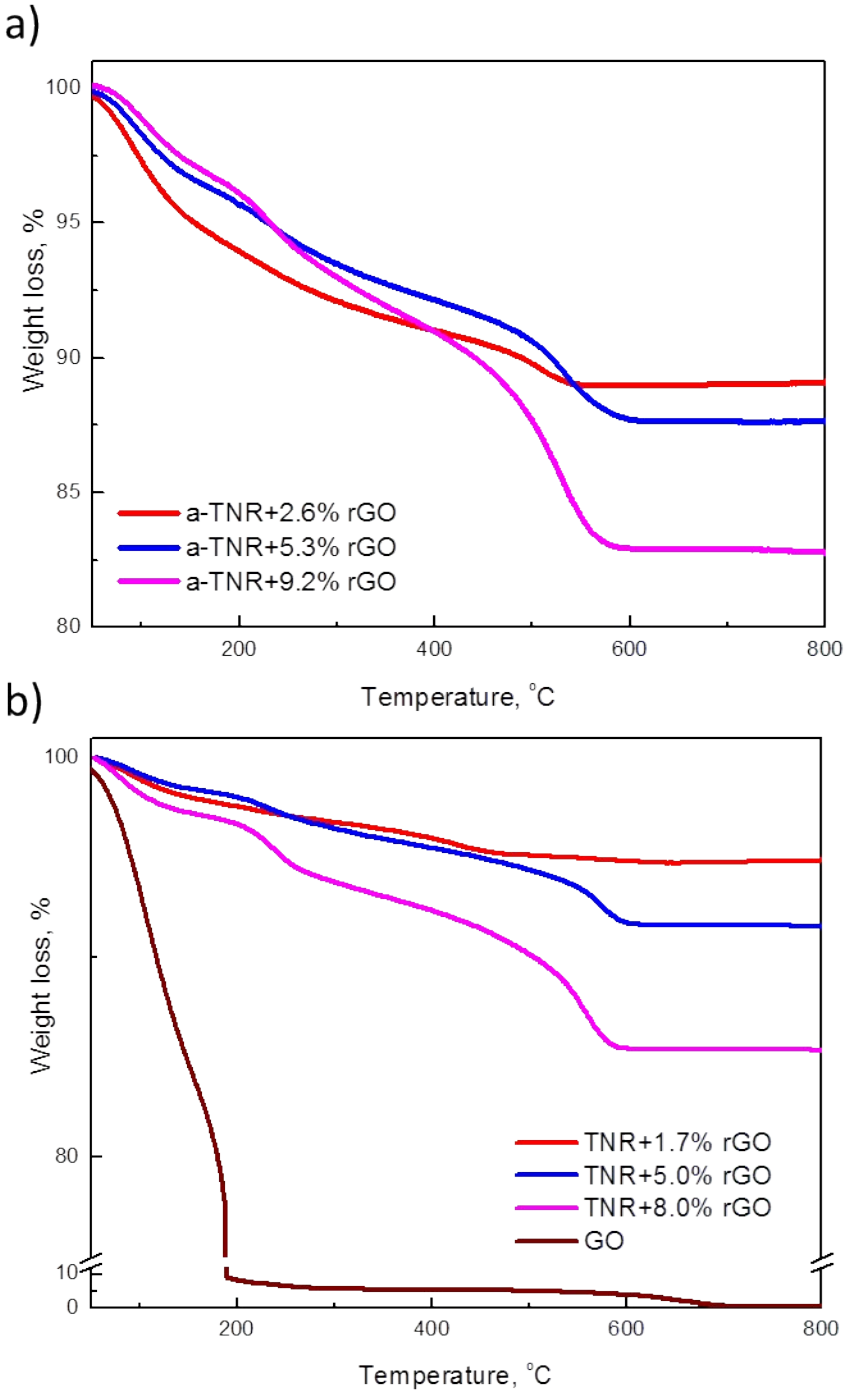

Fig. S3. Thermogravimetric analysis of a-TNR+rGO (a) and TNR+rGO (b) composites as well as of pure GO.

TEM results on graphene

Fig. S4a is showing multilayered thin and dispersed sheets of graphene on amorphous carbon support grid. The transparency of the material is corresponding to the number of graphene layers stacked. Minor curling of the layers is a result of rippling effect. Fig. S4b is showing the SAED pattern taken at the multilayered graphene, the rings correspond to inter-planar distances between individual layers. Here measured d-values are 0.2 nm and 0.11 nm for two strongest reflections. In pure graphite crystals, most intensive reflections are d(002)=0.33 nm and d(101)=0.2 nm [3]. Such observations give us good indication that observed structure is indeed 2D structured graphene and not graphite. The interatomic distances in "hexagon" planes (101) are preserved as shown in Fig. S4c, while the bonds in (002) as shown in Fig. S4d do not exist anymore.

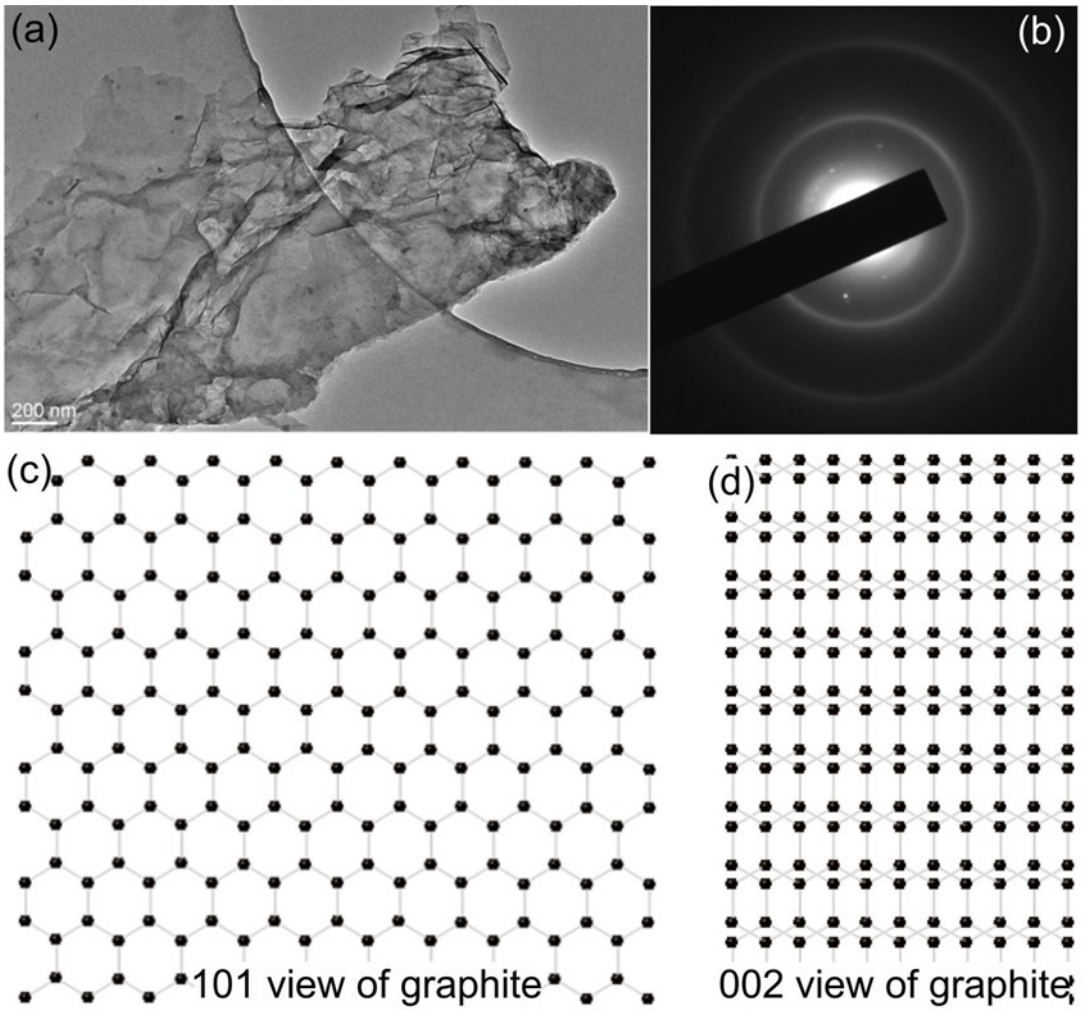

Fig. S4. (a) Multilayered sheets of graphene with small ripples. (b) SAED of multilayered graphene compared with graphite in certain orientation. (c) Graphite view in (101) crystal planes. (d) (002) view of graphite.

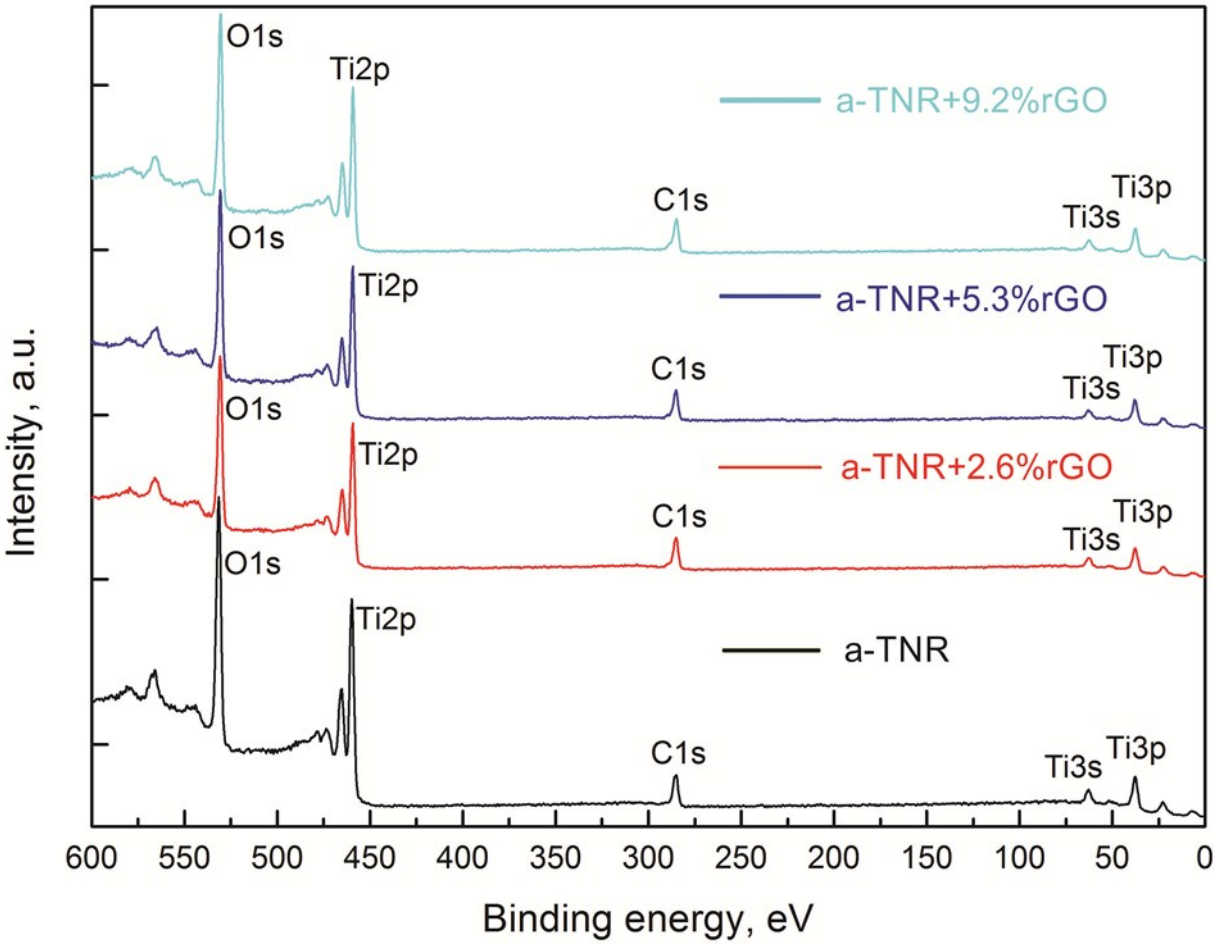

Fig. S5. XPS survey spectrum of GO and a-TNR+rGO composites.

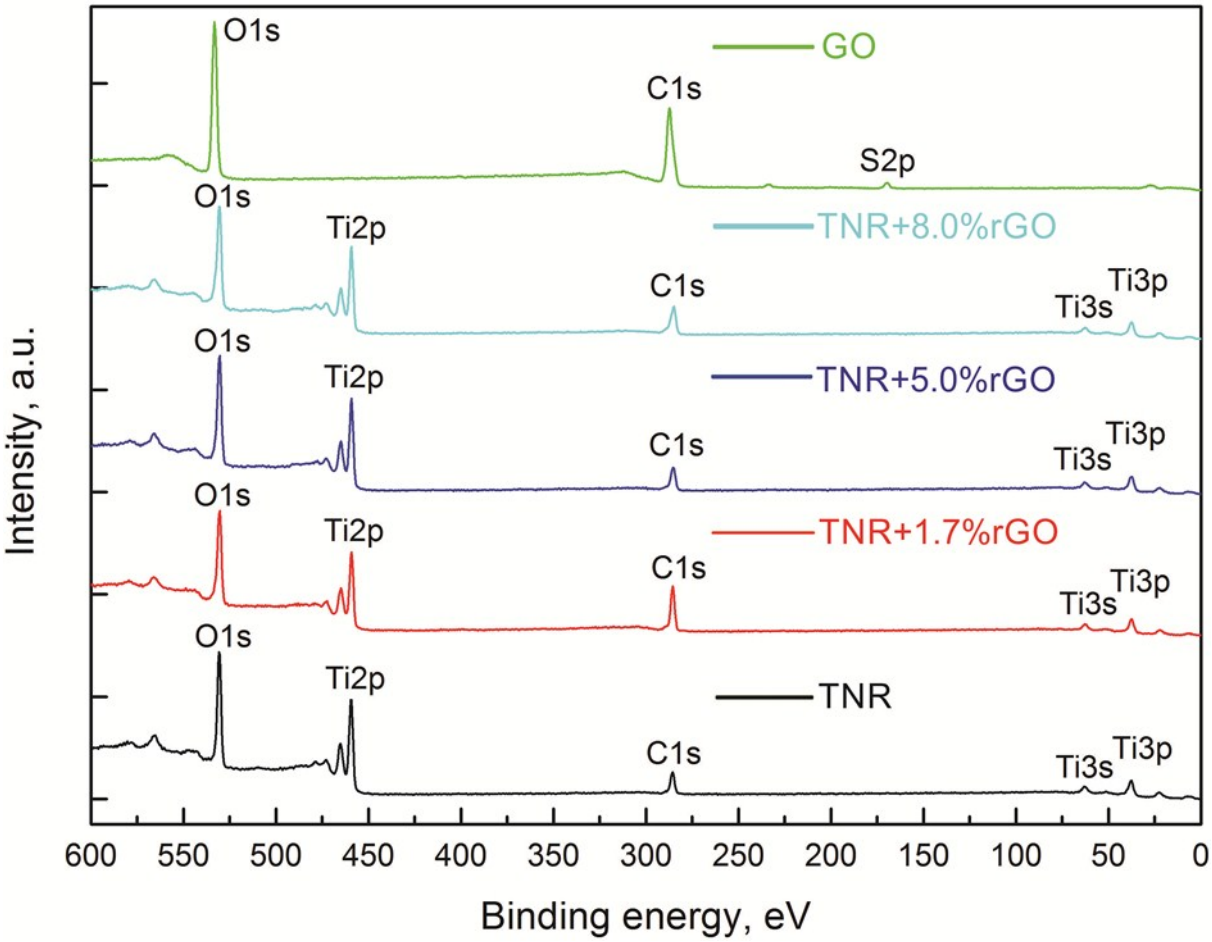

Fig. S6. XPS survey spectrum of GO and TNR+rGO composites.

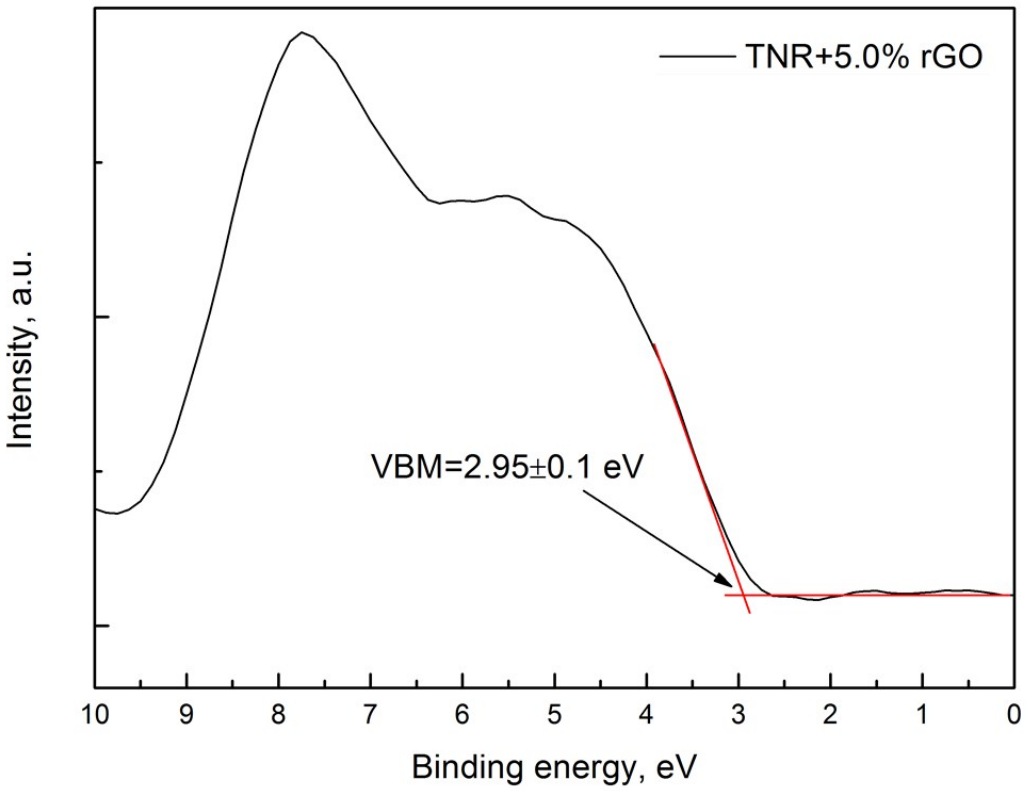

Fig. S7. VBM calculation from XPS data for TNR+5.0% rGO sample.

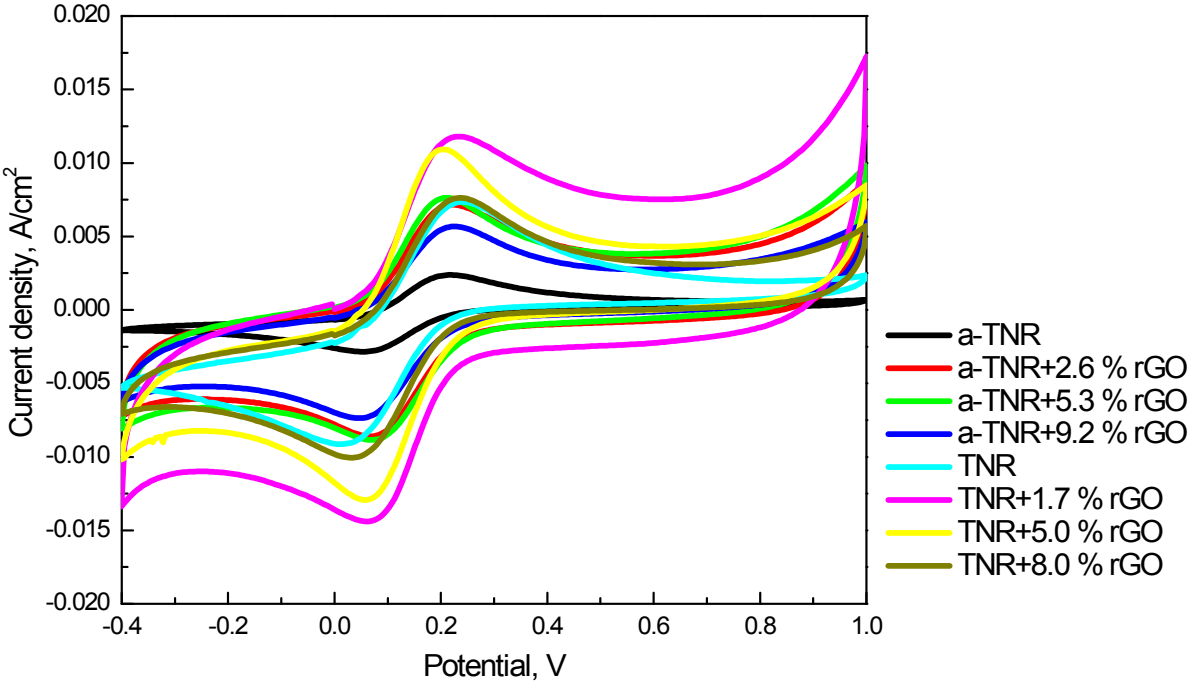

Fig. S8. Cyclic voltammograms recorded for the a-TNR and TNR composites with different amounts of rGO where the specific surface area of the catalysts was considered when calculating the current density.

References

1. S. Lowell, J.E. Shield, M.A. Thomas and M. Thomas, Characterization of Porous Solids and Powders: Surface area, Pore Size and Density, 1st ed., Kluwer Academic Publisher, **2004**.

2. S. Stankovich, D.A. Dikin, R.D. Piner, K.A. Kohlhaas, A. Kleinhamma, Y. Jia, Y. Wu, S.T. Nguyen and R.S. Ruoff, Synthesis of graphene-based nanosheets via chemical reduction of exfoliated graphite oxide, *Carbon*, **2007**, 45, 1558-1565.

3. Y. X. Zhao and I.L. Spain, X-ray diffraction data for graphite to 20 Gpa, *Phys. Rev. B*, **1989**, 40, 993-997.